Communs geol. Surv. Namibia, ***11*** *(1996), 33-48*

U-Pb and Rb-Sr isotopic data for the Mooirivier Complex, Weener Igneous Suite and Gaub Valley Formation (Rehoboth Sequence) in the Nauchas area and their significance for Paleoproterozoic crustal evolution in Namibia

Thomas Becker, Bent Tauber Hansen, Klaus Weber and Bettina Wiegand

Institut für Geologie und Dynamik der Lithosphäre
Goldschmidtstr. 3, D-37073 Göttingen, Germany

U-Pb zircon ages and Rb-Sr whole rock ages have been obtained for several intrusive and volcanic rocks of the Rehoboth Sequence (Weener Igneous Complex, WIC and Gaub Valley Formation, GVF) and the pre-Rehoboth basement (Mooirivier Complex) in the Nauchas area of Namibia. U-Pb zircon upper discordia intercepts define similar ages for the WIC (~1765 and ~1767 Ma), associated granitoids (~1762 Ma and ~1743 Ma), as well as for the pre-Rehoboth Mooirivier Complex (~1725 Ma) and the Neuhof (Kamasis) Formation (~1784 Ma; Burger and Walraven, 1978). These data suggest that the Rehoboth Sequence and the pre-Rehoboth basement are broadly coeval. Rb-Sr whole rock data define errorchrons of ~1752 Ma with an initial $^{87}Sr/^{86}Sr$ ratio of 0.7034 for the GVF and of ~1620 Ma with an initial ratio of 0.7047 for the WIC. An intense disturbance of this isotopic system during post-emplacement alteration processes is inferred.

In a regional context, comparable ages have been determined in crustal segments extending from southern Brazil through southern Africa to equatorial Africa and constitute a major crust-forming event during late Paleoproterozoic times (Eburnian-Ubendian cycle). Similarities in age and rock association of other inliers in Namibia (i.e. Epupa and Huab Inlier, Abbabis Inlier, Namaqua Metamorphic Complex) suggest that much of the pre-Damara basement was formed during this event, in magmatic arc settings.

Introduction

Various magmatic and sedimentary pre-Damara rocks exposed in several inliers along the southern margin of the Damara orogen have been grouped in the past under the sack terms Rehoboth Magmatic Arc (RMA) (Watters, 1976) or Rehoboth Basement Inlier (RBI) (Ziegler & Stoessel, 1993). According to SACS (1980), the respective suites of rocks are subdivided into: (a) high-grade metamorphic complexes and formations of assumed pre-Rehoboth age (Neuhof & Elim Formations, Mooirivier Complex); (b) the ca. 1800 Ma old Rehoboth Sequence (Marienhof, Billstein and Gaub Valley Formations); and (c) the *ca.* 1200 Ma Sinclair Sequence (Nückopf, Grauwater, Eskadron, Doornpoort and Klein Aub Formations). The stratigraphy and regional extent of these pre-Damara units are presented in Table 1 and Figure 1, respectively. This lithostratigraphy is based mainly on field evidence because geochronological data have been absent. However, since most primary contacts between different formations have been overprinted tectonically by the Damara event or earlier orogenies, this classification is preliminary at present. Table 2 shows geochronological data for the pre-Damara units of Namibia. It is obvious that some of the rocks which have been attributed to the Sinclair Sequence are of Rehoboth age and vice versa (i.e. Nückopf, Marienhof, Gaub Valley and Neuhof Formations, Weener Igneous Complex). This is indicative of great petrographic similarities between rocks of different age and probably different origin. Furthermore, besides some poorly defined Sm-Nd ages varying from 1600 to 2600 Ma (Ziegler & Stoessel, 1993) and two doubtful zircon dates, ages older than 1860 Ma have not been recorded in rocks of magmatic origin in this area. Available ages scatter with a bimodal distribution, in the ranges *ca.* 1000 to 1200 Ma and *ca.* 1700 to 1860 Ma, suggesting two distinct magmatic events rather than the continuous crustal reworking proposed by Ziegler and Stoessel (1993).

The stratigraphic and genetic problems outlined above are particularly significant for the volcaniclastic Gaub Valley Formation (GVF) and the Weener Igneous Complex (WIC). The GVF occurs within the Southern Margin Zone of the Damara Orogen as a long NE-SW extending inlier with a total length of 60 km and a maximum width of 20 km (in the type locality), as well as several smaller isolated inliers (Fig. 1). In the past the GVF has been classified as pre-Damara basement, probably older than 1500 Ma (SACS, 1980; Hill, 1975). However, ages between 1000 and 1200 Mahave been obtained on subvolcanic granites (Pfurr *et al.*, 1991) in one of the smaller inliers (Rostock Inlier). Accordingly, these units have been interpreted as either initial rift volcanic rocks of the Damara Sequence or collision-induced rift volcanic rocks of the Sinclair Sequence (Pfurr, 1990). Similar problems apply to the WIC which is intrusive into the GVF and other units of the Rehoboth Sequence (Table 2).

These problems led to a follow-up study of the GVF and WIC in their type localities south of Gamsberg, involving detailed mapping as well as geochemical and isotopic investigations. The possible co-magmatic evolution of the WIC and GVF within a caldera cycle became evident during field work (Becker *et al.*, 1994), a model which required substantiation with isotopic and geochemical data. Results of the isotopic investigation are presented in this paper.

Analytical procedures

Heavy mineral separates were extracted from samples, 20-40 kg in weight, following procedures outlined by Teufel (1988). Zircon concentrates were separated

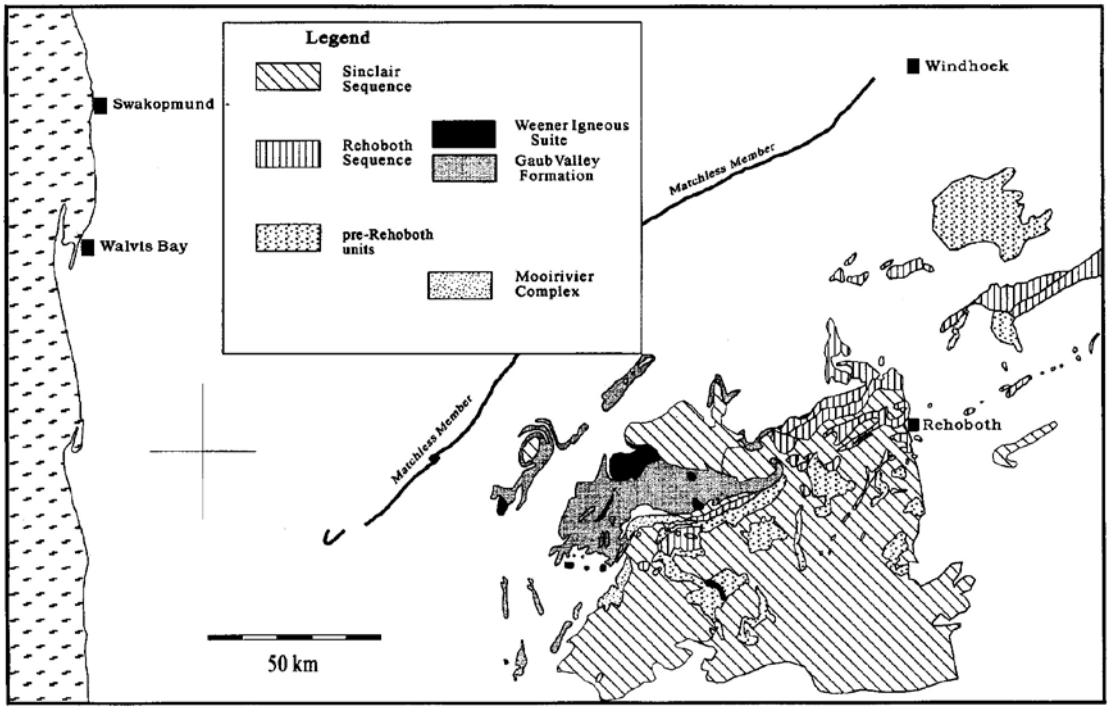

Figure 1: Simplified geological map of the pre-Damara units within the southern Damara Orogen (Matchless Member is shown for orientation)

in fractions of different size and magnetic susceptibility. Only the diamagnetic zircon concentrates were used for further investigation. A selection of 3-5 mg inclusion-poor crystals of each fraction were handpicked for isotope analyses.

The chemical procedures for the zircon analyses followed the method of Krogh (1973). To determine the concentrations of uranium and lead, a highly enriched $^{208}Pb/^{235}U$ mixed spike was added to an aliquot of the zircon solutions. Purification of uranium and lead was carried out on ion exchange microcolumns. Uranium and lead measurements were obtained on a Teledyne 12 inch radius/90° sector mass spectrometer using the rhenium single filament technique. The samples were loaded with Ta_2O_5 (uranium) and H_3PO_4 plus silica gel (lead). Lead isotopic data were corrected for common lead and the analytical blank. The initial lead ratios for the correction of nonradiogenic lead were calculated after the two stage model of Stacey & Kramers (1975) corresponding to an age of 1765 Ma. For age calculations, the constants recommended by IUGS were applied (Steiger & Jäger, 1977). The errors and error correlations in the $^{206}Pb/^{238}U$ and $^{207}Pb/^{235}U$ data were calculated according to Ludwig (1980). They are based on assigned errors of the U-Pb ratio in the spike (0.15%), in the initial ratios $^{207}Pb/^{204}Pb$ and $^{206}Pb/^{204}Pb$ (1 %), in the blank lead (1 %), and its concentration (50%). The correlation factor for initial and blank lead was assigned 0.7. The error ellipses for the data points have been drawn at a confidence level of 95% on the concordia diagrams. A York II regression calculation was used to obtain the ages and errors of intercepts of the best-fit line with the concordia (York, 1969). All errors are given at a 2 σ confidence level.

For Rb-Sr analyses, whole rock aliquots were spiked with a $^{84}Sr/^{87}Rb$ mixed spike prior to dissolution. Separation of Rb and Sr was made by column chemistry using quartz columns filled with cation exchange resin (Bio-Rad* 50 W x 8). The Rb and Sr measurements were made using the tantalum double filament technique

Table 1: Stratigraphy of the pre-Damara units within the southern Damara Orogen (after SACS, 1980).

Sequence	Formation	contact relationship	intrusive unit
Sinclair Sequence	Klein Aub		
		unconformity	
	Doornpoort		
	Eskadron		
		unconformity	
	Grauwater		
	Dordabis		
		disconformity	Gamsberg Granite Suite
	Nückopf		
Rehoboth Sequence	Gaub Valley		Weener Igneous Suite
		unconformity to Marienhof F.	Doornboom Complex
	Billstein	(possibly equivalent to Billstein F.)	Alberta Complex
		unconformity	Swartmodder Granite
	Marienhof		
Pre-Rehoboth units	Elim	correlate of Khoabendus Group	
	Neuhof	closely associated with the Mooirivier C.	Naub Diorite
		unconformity	
	Mooirivier Complex	mainly as xenoliths within the Gamsberg Granite Suite	

for Rb (sample loaded with H_2O^{4*}), and the tantalum single filament technique for Sr (sample loaded with 0.5N $H_3PO_4^{2*}$). Errors based on replicate analyses using standard procedures are 1 % for $^{87}Rb/^{86}Sr$ and 0.01 % for $^{87}Sr/^{86}Sr$. The data for Rb were corrected for mass fractionation compared to standard measurements. For age calculations, the constants recommended by the IUGS (Steiger & Jäger, 1977) were used, with statistical regression calculated according to the method of York (1969). All errors are given at a 2 σ confidence level.

U-Pb zircon ages

Orthogneissic WIC samples have been analysed from the type locality (2), from smaller intrusions within the GVF at distances of 5 and 15 km from the main body (2), and from the Mooirivier Complex (1). Since none of the pyroclastic samples which had been previously collected from the GVF contained zircons, a granitic pebble from the basal clastic-dominated GVF was taken to provide at least a maximum U-Pb zircon age for this formation. The sample positions and their respective U-Pb zircon ages (upper intercept) are shown in figure 2.

Weener Igneous Complex and smaller intrusions within the Gaub Valley Formation

The oval-shaped WIC with dimensions of *ca.* 13 x 7 km is the largest of several tonalitic to granodioritic intrusions in the western part of the Rehoboth area. They are intrusive into the Mooirivier Complex, the Elim and the Gaub Valley Formations, and were in turn crosscut by the Gamsberg and Piksteel Intrusive Suites (Fig. 1, Table 1). Because of similar petrographic characteristics and field relationships, these granitoids were combined as the Weener Igneous Suite by De Waal (1966). However, Rb-Sr age determinations by Reid *et al.* (1988), Seifert (1986) and one U-Pb zircon analysis (one fraction) by Ziegler and Stoessel (1991) on different bodies yielded considerably varying ages of *ca.* 1200 Ma, *ca.* 1870 Ma, and *ca.* 1720 Ma, respectively, probably indicative of several generations of magma genesis.

Two samples were collected from the WIC in its type area south of the Gamsberg. The fine- to medium-grained and variably deformed rocks are clearly of igneous origin, but have been subjected to at least one event of low-grade metamorphism during Pan African (500 Ma) orogeny. Numerous small mafic inclusions and, in some places, large fragments of the country rock

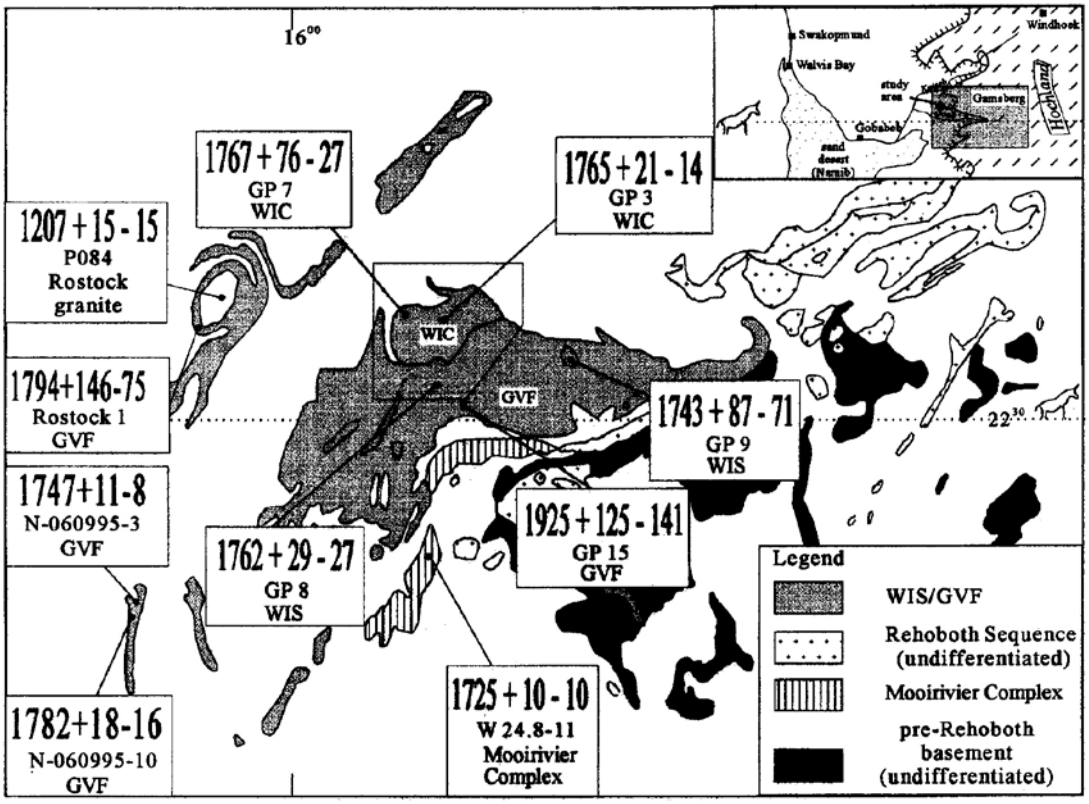

Figure 2: Sample positions and results of the U-Pb isotopic analyses (upper discordia intercepts) of the Weener Igneous Complex, the Gaub Valley Formation and the Mooirivier Complex (ages in Ma). P084 from Pfurr (1990), N-060995 and N-060995-10 from Nagel *et al.* (1996).

are distinctive features. The mineral assemblage comprises quartz, plagioclase and biotite as major components, with varying amounts of hornblende and epidote. Apatite, zircon, chlorite, garnet, muscovite and opaque minerals occur in minor to accessory amounts. Details of the WIC and surrounding lithologies were given by Becker *et al.* (1994) and Becker (1995).

Two samples were taken from smaller granitic intrusions within the GVF (GP8, GP9). Their modal composition is characterized by quartz, two feldspars, biotite and muscovite as major constituents and chlorite, zircon, apatite and ilmenite as minor to accessory phases. The rocks are nearly undeformed and the original magmatic texture is largely preserved. Metamorphism is represented only by grain size reduction of the quartz and the development of high angle grain boundaries. From field evidence it is impossible to attribute these intrusions to the 1200 Ma old Gamsberg Suite or to the older Weener Igneous Suite.

Zircons separated from the two samples of the WIC are homogeneous in typology and composition (Fig. 3). Euhedral prismatic to long prismatic crystals with simple crystal faces are dominant, although many show evidence of magmatic corrosion. In the classification diagram of Pupin (1980), the population covers fields characteristic for zircons derived from mantle magmas, with incipient crystallization temperatures exceeding 900°C. The zircons are light red to colourless and commonly contain inclusions of small randomly oriented crystallites (rounded and euhedral), fluid inclusions and biotite inclusions. In most grains, cathodoluminescence revealed rims with an oscillatory zoning oriented parallel to the c-axis and often small euhedral cores (Fig. 4). These features probably reflect a change in magma composition during growth and a possible inherited component.

Zircon typologies from the granitic intrusions are more variable in comparison to the zircon population of the WIC. In addition to the types described above, there is an important second group characterised by a smaller length/width ratio and a higher degree of metamictisation and corrosion. Inclusion trails and corroded surfaces are attributed to magmatism. Cathodoluminescence revealed the presence of small euhedral dark cores and oscillatory zoning. No metamorphic overgrowths were recognized. .

Results of the isotope analyses are presented in Table 3 and conventional $^{206}Pb/^{238}U$-$^{207}Pb/^{235}U$ concordia diagrams (Fig. 5) after Wetherill (1956). For both WIC samples, similar data have been obtained with low uranium (140-185 ppm) and common lead (0.19-1.24 ppm) concentrations and low degrees of discordance. Therefore, it may be assumed that the isotope system has remained almost undisturbed and the resulting ages probably reflect the time of zircon crystallization. In sample GP3 five size fractions are closely grouped with the coarser fractions having lower concentrations of U and a lower degree of discordance, suggesting that Pb loss was primarily a function of uranium content. The best fit chord (MSWD = 0.99) through the 5 points has intercepts of 1764 +21-14 Ma and 420 ± 250 Ma. Sample GP7 displays a similar pattern with a negative correlation between grain size and uranium concentration as well as degree of discordance. Since the fractions are grouped even more closely than in GP3 the lower intercept is poorly defined and has been constrained at 500 Ma, the time of Damaran metamorphism. Four fractions yielded an upper intercept of 1768 +53-24Ma (MSWD = 0.93). Fraction 3 has been excluded from analysis because of the large deviation from the other data points.

Zircons from the smaller intrusives (GP8, GP9) exhibit higher U (350-620 ppm) and common Pb (2.55-36.74 ppm) concentrations, and a higher degree of discordance compared to the WIC. The higher U concentrations coincide with the more evolved magma composition of these samples. The best fit chords have yielded well defined upper intercepts of 1762 +29-27 and 1743 +87-61 Ma, which are again interpreted as the time of zircon crystallization, and lower intercepts of 49 +57-58 and 55 +136-145 Ma, respectively, indicating Tertiary to Cretaceous Pb loss.

Gaub Valley Formation (GVF)

The Gaub Valley Formation is regarded as the stratigraphically highest unit of the Rehoboth Sequence. It is divided into a clastic dominated lower part and a volcaniclastic upper part. The comagmatic evolution of the GVF and WIC has been inferred from field observations. Since no previously collected volcaniclastic samples from the type locality contain any zircons, a gneissic porphyritic boulder (GP15) from the basal GVF was collected and analysed to provide constraints on the age of the provenance and the maximum age for the GVF .

The idiomorphic transparent zircons of this sample are again prismatic to long prismatic with simple crystal faces, and varying in colour from colourless to light red. Cathodoluminescence revealed a zoning and the presence of small euhedral cores. However, the isotopic data differ from those obtained for the previous samples with respect to an increased fraction of common Pb (up to 48.2%), and accordingly a large error in the age calculations. Within the fractions 2 to 5 the grain size correlates negatively with U concentration and degree of discordance but not with common Pb. In the concordia diagram the best fit chord (MSWD = 0.428) has poorly defined upper and lower intercepts of 1929 +125 -141 Ma and 439 +125 -141 Ma, respectively.

Additionally, three volcaniclastic samples of the GVF have been analysed from smaller inliers of the Rostock and Saagberg area (Fig. 2) (Nagel *et al.*, 1996). In the concordia diagram the upper discordia intercepts are 1794 + 146-75 Ma (MSWD = 0.19),1747 +11-8 Ma (MSWD = 2.8) and 1782 +18 -16 Ma (MSWD = 7.69), and have been interpreted as time of crystallization. The

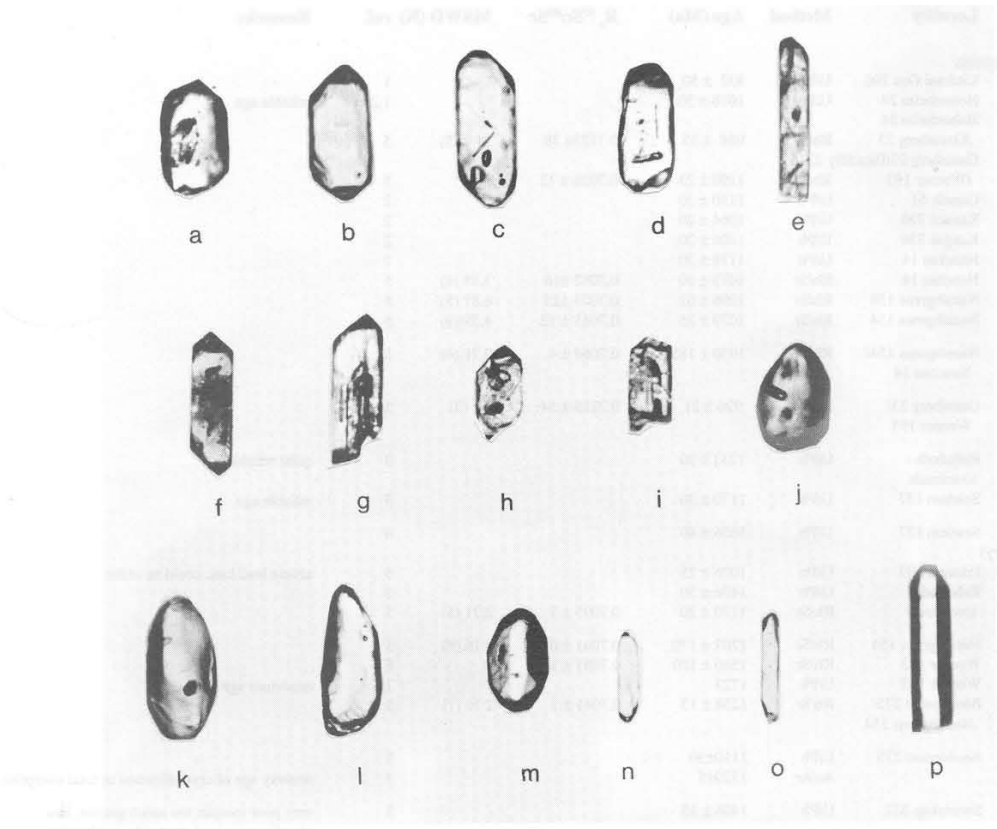

Figure 3: Zircon typologies of samples GP3 and GP7. a-e: clear, idiomorphic; f-i: idiomorphic with small inclusions; j-m: clear, rounded; n-p: clear, long prismatic crystals.

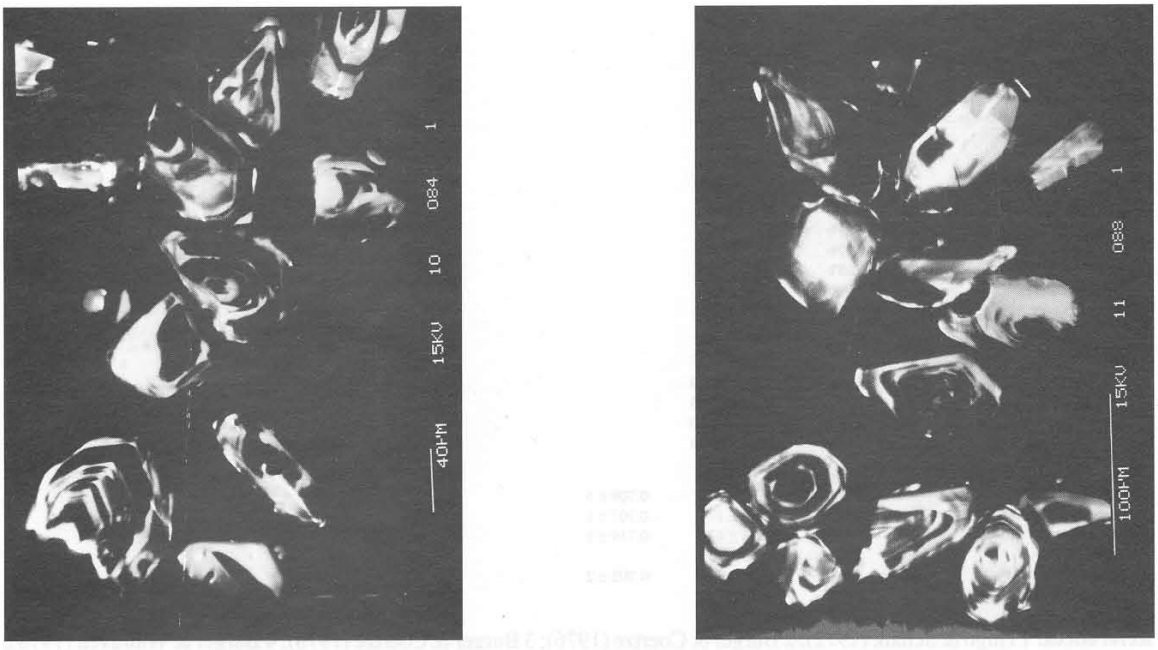

Figure 4: SEM photographs of polished crystals (cathodoluminescence mode), showing small rounded to euhedral cores and zoned rims.

Table 2: Geochronological data for the pre-Damara units of Namibia and neighbouring areas.

Lithological unit	Locality	Method	Age (Ma)	R_o $^{87}Sr/^{86}Sr$	MSWD (N)	ref.	Remarks
Central Namibia							
	Uitdraai Oos 296	U/Pb	932 ± 50			1	
	Hohenheim 24	U/Pb	1078 ± 30			1,2	reliable age
	Hohenheim 24 /Gamsberg 23	Rb/Sr	984 ± 55	0.7123± 39	21.0 (5)	5	
Gamsberg	Gamsberg 23/Picadilly 221 /Weener 193	Rb/Sr	1190 ± 23	0.7026 ± 12		5	
Granite	Ganeib 61	U/Pb	1150 ± 30			2	
	Kanaus 336	U/Pb	1064 ± 20			2	
Suite	Kangas 336	U/Pb	1104 ± 20			2	
	Nauchas 14	U/Pb	1178 ± 20			2	
	Nauchas 14	Rb/Sr	1073 ± 20	0.7082 ±16	3.48 (4)	5	
	Namibgrens 154	Rb/Sr	1096 ± 62	0.7075 ±25	6.87 (5)	5	
	Namibgrens 154	Rb/Sr	1079 ± 25	0.7081 ± 12	4.39 (9)	5	
Post-Gamsberg mafic dykes	Namibgrens 154/ Nauchas 14	Rb/Sr	1030 ± 185	0.7064 ± 4	0.71 (4)	5	
Post-Gamsberg aplites	Gamsberg 23/ Weener 193	Rb/Sr	926 ± 21	0.7215 ± 54	(3)	5	
Marienhof F. (acid lava)	Rehoboth - townlands	U/Pb	1232 ± 30			3	quite reliable
rhyolite	Sesriem 137	U/Pb	1170 ± 30			3	reliable age
Barby F. (quartz porphyry)	Sesriem 137	U/Pb	1656 ± 40			4	
Piksteel Suite	Piksteel 209	U/Pb	1076 ± 25			3	severe lead loss, could be older
	Rehoboth - townlands	U/Pb	1476 ± 30			2	
		Rb/Sr	1170 ± 20	0.7095 ± 7	2.21 (5)	5	
Weener Igneous Complex	Namibgrens 154	Rb/Sr	1207 ± 170	0.7041 ± 6	0.16 (5)	5	
	Weener 193	Rb/Sr	1560 ± 100	0.7051 ± 14		6	
	Weener 193	U/Pb	1723			7,8	minimum age
	Biesiepoort 275/ Namibgrens 154	Rb/Sr	1238 ± 13	0.7041 ± 1	2.16 (7)	5	
Biesiepoort granite	Biesiepoort 275	U/Pb	1110±30			3	
		Ar/Ar	1529±5			3	primary age of crystallization or total overprint
Kam Kam	Swartskap 332	U/Pb	1406 ± 35			3	very poor sample, too much granite, loss of radiogenic lead, probably much older
	Kam Kam 369	U/Pb	986 ± 20			3	minimum age, possibly higher - loss of lead
Kamasis F. (acid lava)	Olivantsvloer 453	U/Pb	1328 ± 25			4	minimum age
Kamasis F.	Neuras 330	U/Pb	1784 ± 45			4	reliable minimum age
Granite	Rehoboth village	U/Pb	1784 ± 45			4	reliable minimum age
Neuhof F.	Hebron 136	U/Pb	1294 ± 25			3	minimum age, could be much older
Abbabis Complex	Central Namibia	U/Pb	1925 ± 300			15	
Kheis Tectonic Province							
Groblershoop Schist F.		U/Pb	1780			9	
Nückopf F. (porphyry)	Auchas 347	U/Pb	1770 ± 35			3	a minimum age at least
Dagbreek F.		U/Pb	1800-2100			10	inherited age
Hartley Andesite F.	Rb/Sr		2026 ± 180	0.7044 ± 3		11	
Outjo district							
Acid lava	Suiderkruis 668	U/Pb	1765 ± 40			2	
Granite	Annabis 677	U/Pb	1815 ± 40			2	
Granodiorite		U/Pb	1850 ± 40			2	
Porphyry Granite		U/Pb	1860 ± 40			2	
Quartz porphyry		U/Pb	1860 ± 40			2	
N. Namibia							
Fransfontein Suite		K/Ar	±2100			12	
Epupa Complex		U/Pb	1795+33/-29			13	
Huab Complex		U/Pb	1811+39/-35			13	
Post-Huab Granitic Gneiss		U/Pb	1749+78/-70			13	
Oas Syenite		U/Pb	2124+68/-54			13	inherited age
Namaqua Metamorphic Complex - S. Namibia							
Tsams/Hom F.		Rb/Sr	1658 ± 280	0.709 ± 5		14	
Khurisberg Subgroup		Rb/Sr	1848 ± 174	0.707 ± 1		14	
Vioolsdrif Suite		Rb/Sr	1676 ± 42	0.719 ± 1		14	
Vioolsdrif Suite		Pb/Pb	1839 ± 58			14	
Gladkop Suite		Rb/Sr	1824 ± 70	0.705 ± 2		14	
Gladkop Suite		Pb/Pb	1770 ± 187			14	

References: 1 Hugo & Schalk (1972); 2 Burger & Coertze (1976); 3 Burger & Coertze (1978); 4 Burger & Walraven (1978); 5 Reid *et al.* (1988); 6 Seifert (1986); 7,8 Ziegler & Stoessel (1991, 1992, 1993); 9 Moen (1976); 10 Barton & Burger (1983); 11 Crampton (1974); 12 De Carvalho (1970); 13 Tegtmeyer & Kröner (1985); 14 Barton (1983); 15 Jacob *et al.* (1978)

Table 3: Results of zircon analyses.

sample	fraction	concentration				measured ratios				calculated ratios		calculated ages (2-stage model, Stacey & Kramers, 1975)		
	[µm]	U [ppm]	Pb^{tot} [ppm]	Pb^{rad} [ppm]	Pb^{com} [ppm]	$^{206}Pb/^{204}Pb$	$^{207}Pb/^{206}Pb$	$^{208}/^{206}Pb$	$^{206}Pb/^{238}U$	$^{207}Pb/^{235}U$	$^{207}Pb/^{206}Pb$	$^{206}Pb/^{238}U$	$^{207}Pb/^{235}U$	$^{207}Pb/^{206}Pb$
GP3/1	>100	174	56.49	55.6	0.87	2828	0.11162	0.17698	0.29254	4.3078	0.11162	1654	1695	1746
GP3/2	80-100	178	56.74	56.4	0.37	5451	0.10909	0.16481	0.29119	4.2794	0.10908	1648	1689	1741
Gp3/3	60-80	178	57.02	56.4	0.58	4146	0.10977	0.16839	0.29087	4.2705	0.10977	1646	1688	1740
Gp3/4	45-60	186	58.50	58.2	0.29	6269	0.10864	0.16551	0.28669	4.2084	0.10864	1624	1675	1739
Gp3/5	<45	186	58.64	58.3	0.39	5925	0.10884	0.17068	0.28624	4.2047	0.10883	1623	1675	1741
Gp7/1	>100	154	50.27	49.4	0.92	2490	0.11207	0.18916	0.28938	4.2535	0.11207	1638	1684	1742
Gp7/2	80-100	162	52.05	51.4	0.66	3426	0.11034	0.18267	0.28809	4.2251	0.11034	1632	1679	1738
Gp7/3	60-80	139	45.27	44	1.24	1361	0.11519	0.19591	0.28865	4.1854	0.11519	1635	1671	1717
Gp7/4	45-60	165	52.60	52.4	0.19	4013	0.10973	0.18872	0.28685	4.2055	0.10973	1626	1675	1737
Gp7/5	<45	160	50.85	50.5	0.33	2868	0.11121	0.19012	0.28544	4.1894	0.11121	1619	1672	1740
Gp8/1	>100	351	106.48	69.7	36.74	109	0.23236	0.45169	0.18389	2.7308	0.10647	1088	1337	1761
Gp8/2	80-100	400	79.36	75.5	3.87	925	0.12133	0.15412	0.17896	2.63016	0.12133	1061	1309	1742
Gp8/3	60-80	424	80.86	77.8	3.05	1164	0.11829	0.14598	0.17422	2.56021	0.11828	1035	1289	1741
Gp8/4	45-60	501	88.36	85.2	3.21	1093	0.1187	0.14693	0.1618	2.33699	0.1187	967	1234	1736
Gp8/5	<45	538	93.22	90.7	2.55	1231	0.11749	0.14514	0.16015	2.34975	0.11749	958	1227	1739
Gp9/1	>100	324	81.12	68.3	12.82	259	0.15642	0.43385	0.17265	2.4657	0.15642	1026	1262	1689
Gp9/2	80-100	471	91.89	82.4	9.48	433	0.13566	0.33987	0.14807	2.1249	0.13566	890	1156	1698
Gp9/3	60-80	553	105.44	98.2	7.21	625	0.12685	0.30772	0.15145	2.1925	0.12685	909	1178	1714
Gp9/4	45-60	606	120.00	113	6.83	764	0.12322	0.29899	0.15914	2.3118	0.12322	952	1216	1721
Gp9/5	<45	620	124.11	117	7.51	706	0.12414	0.30887	0.15957	2.306	0.12414	954	1214	1711
W28.8-11/1	>100	793	164.29	162	2.06	2726	0.10449	0.08512	0.20319	2.7858	0.10449	1192	1352	1614
W28.8-11/2	80-100	754	159.64	158	1.89	3598	0.1038	0.0869	0.20668	2.8492	0.1038	1211	1368	1623
W28.8-11/3	60-80	724	154.93	155	0.06	3215	0.10429	0.09063	0.21095	2.9089	0.10429	1233	1384	1624
W28.8-11/4	45-60	626	143.02	141	1.80	3848	0.10453	0.09611	0.22068	3.07208	0.10453	1285	1426	1642
W28.8-11/5	<45	562	134.12	133	1.43	4089	0.10493	0.10455	0.22934	3.2121	0.10493	1331	1460	1653
W24.8-11/6	>100	763	160	157	2.5	3750	0.10411	0.08606	0.2035	2.81827	0.10044	1194	1360	1632
W24.8-11/7	80-100	718	154.48	152	2.18	3963	0.1043	0.08857	0.20903	2.90624	0.10084	1224	1384	1640
GP15/1	>100	658	175.30	116	59.40	116	0.21734	0.49081	0.15562	2.11602	0.09862	932	1154	1598
GP15/2	80-100	796	218.12	141	77.14	109	0.22444	0.51131	0.15606	2.11931	0.09849	912	1133	1585
GP15/3	60-80	547	159.74	111	48.99	116	0.20648	0.4584	0.17859	2.51845	0.10227	1059	1277	1666
GP15/4	45-60	441	136.37	91.6	44.76	120	0.21853	0.47941	0.18318	2.65327	0.10505	1084	1316	1715
GP15/5	<45	398	188.70	97.7	91.01	70	0.30287	0.68884	0.21241	3.14297	0.10732	1242	1443	1754

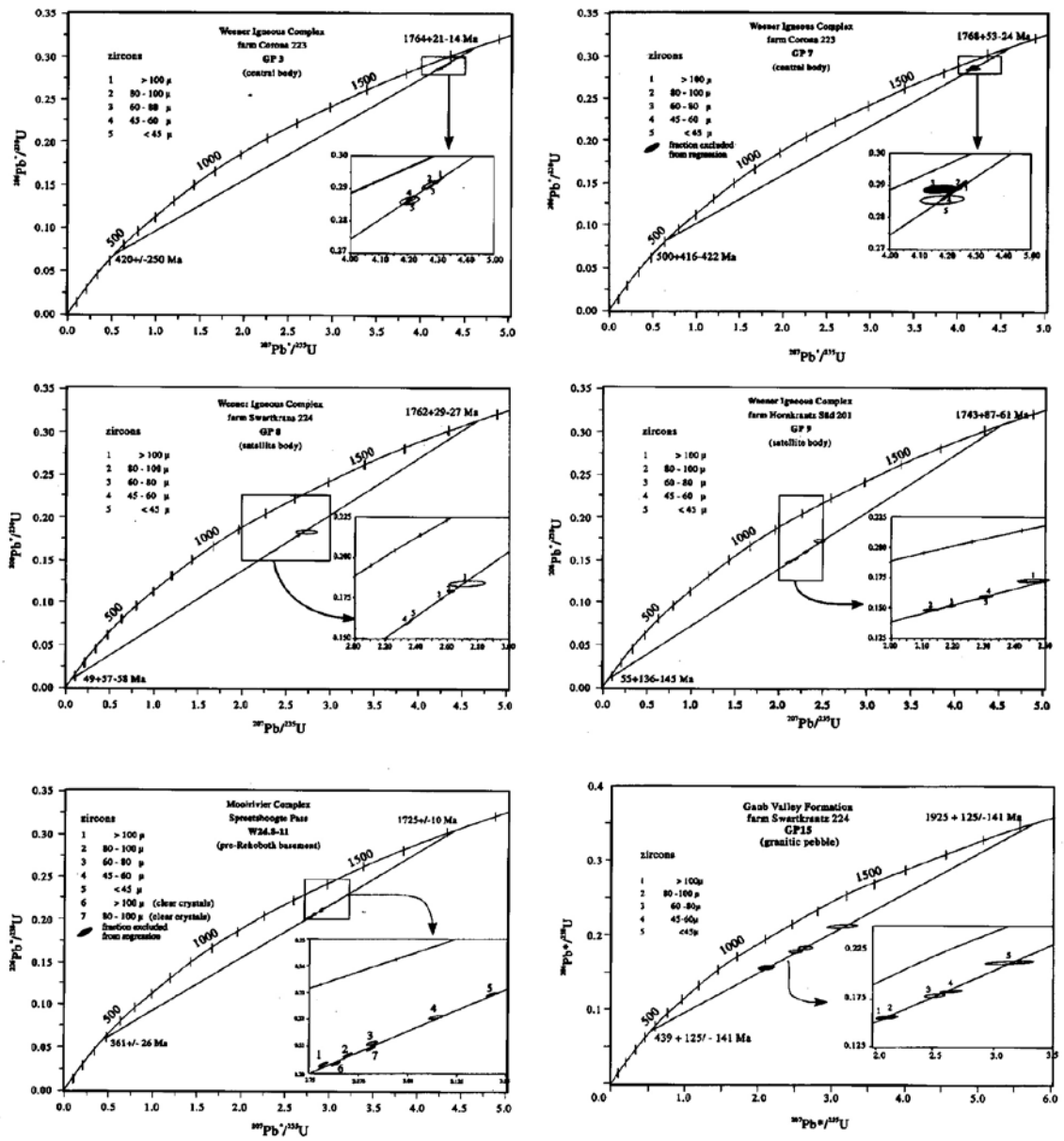

Figure 5: Concordia diagrams for zircons of the analysed samples

poorly defined lower discordia intercepts vary between 386 ± 159 Ma and 325 ± 54 Ma.

Mooirivier Complex

The Mooirivier Complex has been considered to represent the oldest crustal segment in the Southern Margin Zone (SMZ) of the Damara Orogen (Schalk, 1988). The name applies to a whole group of highly metamorphosed rocks mainly preserved as large schollen within younger granitoid intrusives, which have not been previously investigated by means of isotopic or geochemical analyses. Their widespread distribution in numerous small outcrops throughout the whole SMZ attests to the wide area previously underlain by this basement. Intensely folded migmatitic gneiss and amphibolite, together with remnants of quartzite and schist, are the main lithotypes of this unit (SACS, 1980). In its eastern portion the Mooirivier Complex is closely associated with the volcanic Kamasis Formation.

The sample for the zircon study (W.24.8-11) was taken from the largest outcrop at the Spreetshoogte pass (Fig. 2). This gneissic rock with incipient migmatization structures is clearly of igneous origin and intruded the surrounding metabasites parallel to foliation planes. The succession was in turn intruded by younger granitoids, probably of Sinclair age.

Two groups of zircons are distinguished in this sample. The dominant group comprises subhedral prismatic, metamict, yellow to reddish strongly corroded

zircons. Cathodoluminescence reveals the presence of homogeneous rounded to euhedral cores, with overgrowths exhibiting oscillatory zoning. Corrosion of the zircons is indicated by rugged crystal surfaces, and by cracks and tubes within the crystals. The second group displays similar features as described from zircons of the other samples with transparent euhedral prismatic to long prismatic zircons and simple crystal faces (Fig. 6). In contrast to the first group, these specimens are only slightly corroded. Internal structures such as rounded or subhedral cores and overgrowths with oscillatory zoning are recognizable (Fig. 7).

Five fractions from the first and two fractions from the second group have been analysed. In contrast to the other samples, the grain size correlates positively with U concentration (562-793 ppm), degree of discordance, and in general also with common Pb (0.06-2.06 ppm) (Fig. 5). The fractions from the first group define well constrained upper and lower intercepts of 1725 ± 10 Ma and 361 ± 26 Ma (MSWD = 2.99). Both size fractions from the second group are grouped close to the corresponding fraction of the first group and display similar geochemical characteristics (Fig. 5, Table 3). Discordia intercepts are 1721 +36-31 Ma and 303 +89-92 Ma.

Rb-Sr whole-rock ages

Rb-Sr isotopic data have been determined for 5 samples from the WIC and 6 from the GVF. Analytical data are given in Table 4.

Since the variation of the Rb/Sr-ratio is low in the WIC (0.14-0.35), increased errors are inherent a prior to the regression analysis. To improve the significance of the calculated age, previously published analyses from the same locality (Seifert, 1986) have been included. Due to their large deviation from the regression line, two samples have been excluded (KAW 2287, PR18). Even so, the remaining 9 samples poorly define an errorchron (MSWD = 21, Fig. 8) with an age of 1655 ± 123 Ma and an initial $^{87}Sr/^{86}Sr$ ratio of 0.7041 ± 13.

The Rb-Sr whole-rock data for the GVF are plotted in figure 9. Most of $^{87}Rb/^{86}Sr$-ratios are comparable to those in the WIC. The tendency to increased Rb/Sr-ratios (0.16-0.95) coincides with a higher degree of differentiation of the volcanic rocks (Becker *et al.*, in prep.). Five samples define an errorchron (MSWD = 28.2) with an age of 1760± 123 Ma and an initial $^{87}Sr/^{86}Sr$ ratio of 0.7033± 13. However, sample VU11 is distinct from the others in both a higher Rb/Sr ratio and a large negative deviation from the regression line. Supposing an origin from a depleted mantle source for this sample, a maximum model age of 1246 Ma would result. Additional crustal contamination will lead to further rejuvenation. The geochemical analysis of this sample shows an anomalous composition in comparison with the other samples (Becker *et al.*, in prep.). Therefore, a different

Table 4: Results of Rb-Sr whole rock analyses.

lithological unit	sample	concentration		measured ratios		
		Rb [ppm]	Sr [ppm]	Rb^{87}/Sr^{86}	Sr^{87}/Sr^{86}	2MQFM
this study						
	PR04	98.70	298.21	0.95939	0.7267808	0.0000434
	PR10	51.28	359.83	0.412586	0.7140362	0.0000439
WIC	PR13	88.44	317.89	0.80611	0.722662	0.0000939
	PR16	65.79	288.19	0.661329	0.721079	0.0000863
	PR18	50.49	311.60	0.469266	0.717531	0.0003111
	VU08	45.92	281.37	0.47248	0.714873	0.0000701
	VU09	67.39	326.44	0.597894	0.718873	0.0000519
	VU10	97.22	247.44	1.139657	0.734053	0.000138
GVF	VU11	184.43	81.58	6.613083	0.820357	0.0001228
	VU20	125.96	149.59	2.44904	0.761979	0.0000867
	VU22	72.93	243.07	0.869567	0.725065	0.000117
SEIFERT (1986)						
	KAW2282	97.81	273.41	1.019921	0.727762	0.000085
	KAW2287	109.39	319.10	0.976854	0.723074	0.000079
	KAW2288	88.35	245.12	1.027771	0.729274	0.00006
WIC	KAW2289	79.30	337.91	0.668411	0.718556	0.00005
	KAW2290	90.32	243.18	1.058944	0.729032	0.000095
	KAW2291	90.22	321.09	0.80068	0.72311	0.000053
regression error				1%	0.01%	

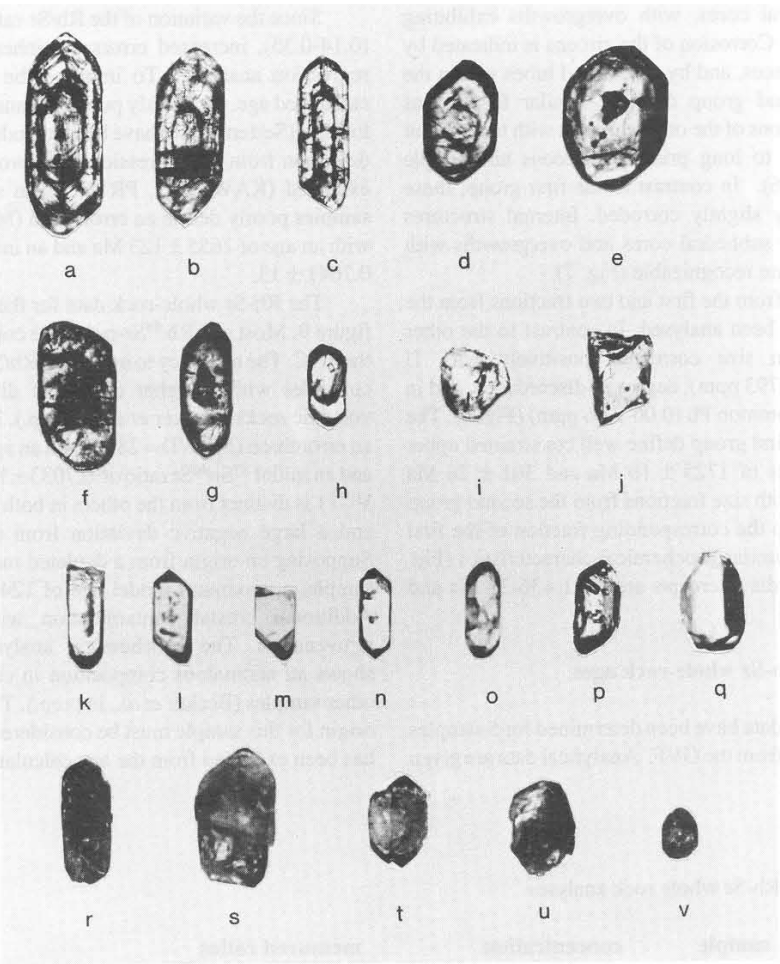

Figure 6: Zircon typologies of sample W24.8-11: a-e: zoned idiomorphic f-j: anhedral to euhedral with cores, k-q clear, unzoned, some with inclusions, r-v: metamict crystals

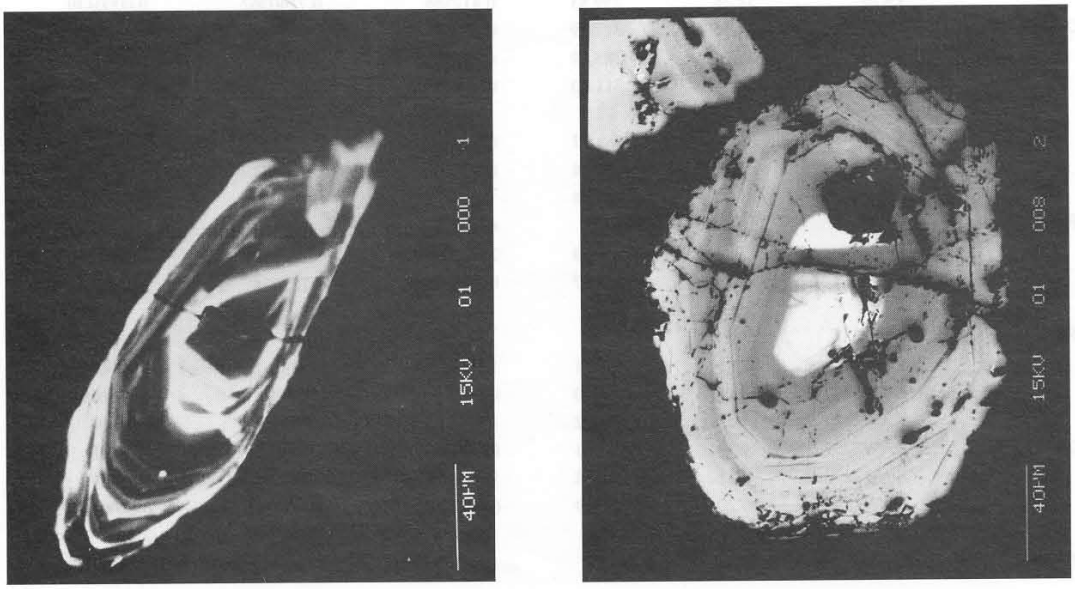

Figure 7: SEM photographs of polished crystals (cathodoluminescence mode), a) zoned zircon of the first group with small euhedral core and holes and microchannels throughout the crystal, b) zoned zircon of the second group.

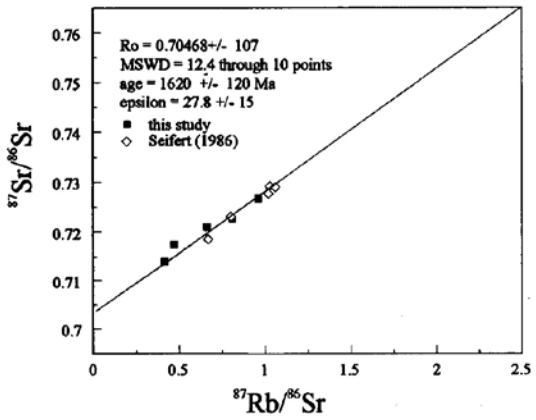

Figure 8: Rb-Sr errorchron diagram of the Weener Igneous Complex.

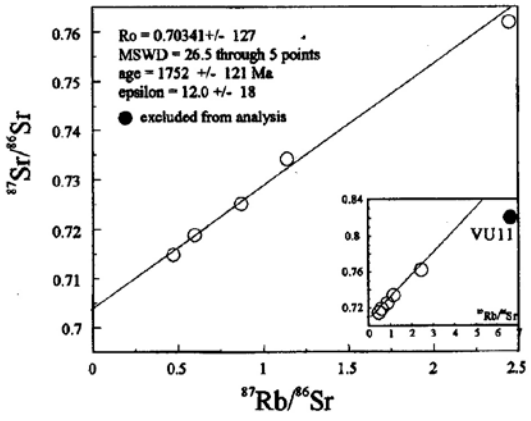

Figure 9: Rb-Sr errorchron diagram of the Gaub Valley Formation.

origin for this sample must be considered and accordingly it has been excluded from the age calculation.

Discussion

U-Pb intercept ages

In the Concordia diagrams after Wetherill (1956) most zircon fractions define discordant chords as a result of radiogenic lead loss. The relationships between the incorporation of common lead, lead loss (expressed in the ratio $^{207}Pb/^{235}U$) and uranium concentration is shown in figures 10 and 11. In most of the samples the uranium concentration and degree of discordance are negatively correlated. Additionally, the sample from the Mooirivier Complex deviates significantly from the regression curve defined by the other samples. This shows, that the loss of radiogenic lead is partly controlled by the uranium concentration. The susceptibility of zircons to lead loss as a function of radiation damage has already been pointed out by Ludwig and Stuckless (1978). However, the mechanism for different degrees of lead loss at different localities remains unknown. Figure 11 shows that in four samples only very low common lead concentrations occur and any correlation will probably be blurred by the analytical error. A negative correlation between uranium and common lead has only been observed in the samples with higher common lead concentrations. Again, the incorporation of common lead into the zircons is only partly controlled by radiation damage and hence an unknown factor must have led to different degrees of exchange at different localities.

For the samples from the WIC and associated smaller intrusive bodies the upper intercept ages range with low 2-sigma errors from 1743 to 1768 Ma. Most of the zircons have remarkably small euhedral cores and broad oscillatory zoned rims. This is taken as evidence for the origin of the crystals in only one magmatic event while the influence of any inherited component is probably negligible. In conclusion, these ages are interpreted as

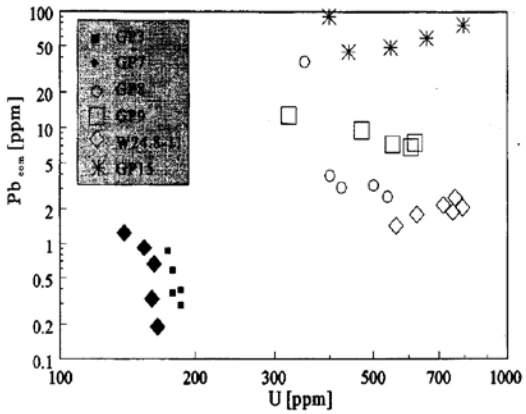

Figure 10: Pb_{com} vs. U diagram of all zircon analyses.

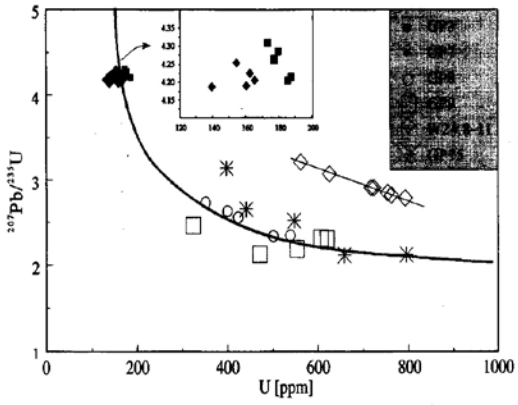

Figure 11: Discordance (expressed as $^{207}Pb/^{235}U$) vs. U diagram of all zircon analyses.

the times of crystallization. A mantle origin of the parental magma is indicated, in application of the classification diagram of Pupin (1980) by simple crystal faces, and additionally supported by the low uranium concentration in the zircons.

In the orthogneissic sample from the Mooirivier Complex, two zircon groups are distinguished. Narrow-spaced broad oscillatory rims attest to the dominant magmatic origin of both groups. In some grains, an inherited sedimentary component is indicated by rounded cores. The coexistence of the two groups may be explained in two ways:

1. the different degrees of metamictization and corrosion are the result of increasing uranium concentrations and may be related to differentiation and mixing of more differentiated magma with early fractionates;
2. the strongly corroded zircons of the first group are evidence for a hybrid magma. These orthogenic xenocrysts were assimilated from the country rock during magma ascent.

The first model is favoured since metamict zircons are much more abundant than clear ones, and because transitions between the two groups have been observed. This model also accounts for the similar upper intercepts of 1725 and 1721 Ma. Altogether this age is rather surprising since the Mooirivier Complex is believed to represent the basement of the Rehoboth Sequence and therefore should yield considerably older ages. Several models could explain this apparent discrepancy:

1. the Mooirivier Complex is coeval with the Rehoboth Sequence and only represents a deeper level of the same crustal segment;
2. the Mooirivier Complex is indeed older than the intrusive rock which had been analysed. The zircon age only provides a minimum age;
3. thermal overprint and isotopic rehomogenisation of the zircons during a high-grade metamorphic event which is indicated by the incipient migmatitic structures.

Since reliable U-Pb zircon ages have not been recorded from the SMZ which attest to basement older than 1860 Ma, the first possibility seems most likely. A similar zircon age of 1784 ± 45 Ma has been obtained from the volcanic Kamasis Formation which is closely associated with the Mooirivier Complex. This age has been interpreted as the time of crystallization (Burger & Walraven, 1979; SACS, 1980; Schalk, 1988).

In conclusion, at present the pre-Rehoboth basement and the Rehoboth Sequence cannot be distinguished on the basis of absolute ages. The different degree of metamorphism and/or additional deformation structures in pre-Rehoboth units as compared to the Rehoboth Sequence do not argue for an earlier origin and may rather result from burial to different crustal levels during later metamorphism. A major thrust system that could have brought units from different crustal positions into juxtaposition is the Areb Shear Zone, which is believed to be of pre-Sinclair age (Schulze-Hulbe, 1979).

The upper intercept of zircons from a magmatic pebble within the clastic GVF is poorly defined, with a large uncertainty in this age caused by the exceptionably high contamination of zircons with common lead. The calculated age of 1929 +125 -141 Ma does not significantly constrain the maximum age of the GVF nor the age of the provenance area. It is the oldest U-Pb zircon age so far obtained in the Southern Margin Zone. However, the $^{207}Pb/^{206}Pb$ ages of the different fractions vary within the same range as the remainder of the analysed samples and do not exceed 1754 Ma (Table 3). A similar poorly defined U-Pb zircon age of 1925 ± 280 Ma has been reported from the Abbabis Inlier which is situated north of the SMZ in the Central Zone of the Damara belt (Jacob *et al.*, 1978). Finally, upper discordia intercepts of 1794 + 146 -75 Ma, 1747 + 11-8 Ma, and of 1782 +18 -16 Ma from pyroclastic samples of the GVF in the Rostock and Saagberg areas, interpreted as time of crystallization, clearly attest to the more or less coeval evolution of the GVF and the WIC (Nagel *et al.*, 1996).

Due to high 2-sigma errors in most of the samples the lower intercepts are difficult to assess. Various geological events are documented by other methods during which episodic lead loss may have occurred. The *ca.* 1200 Ma Sinclair magmatism is regarded as a first regional magmatic event resulting in high-level intrusions with contact metamorphism and basic and acid volcanism. However, no significant disturbance of the U-Pb isotope system is indicated during this time. This is indicated by the data from the WIC which are only slightly discordant despite the proximity of the sample localities to intrusions of Sinclair age (i.e. Gamsberg Granite Suite).

The *ca.* 500 Ma Damara metamorphism probably had a strong effect on the isotope systematics in the SMZ. A compilation of biotite and muscovite isotopic ages (Fig. 12) reveals that K/Ar and Rb/Sr mineral ages of muscovite scatter within a comparatively narrow range between 475 and 525 Ma, whilst the biotite ages were rejuvenated up to 350 Ma. This rejuvenation has been attributed to a hydrothermal event which is recorded by the observed full age spectrum in samples taken only meters apart at Gamsberg Mountain (Seifert, 1986).

A combination of zircon populations from the WIC with low uranium concentrations and low degrees of discordance (i.e. GP3, GP7) fits on a discordia with a lower intercept of 528 ± 163 Ma and may represent the original episodic chord for Damaran metamorphism.

The hydrothermal event possibly is also documented in the sample from the Mooirivier Complex. The lower discordia intercept of 362 ± 27 Ma is in good agreement with K-Ar biotite ages of 347 ± 4 Ma and 357 ± 4 Ma from the same locality (Ziegler & Stoessel, 1993), and with zircon fission track ages of 372 ± 35 and 359 ± 42 Ma from the Gamsberg area (Seifert, 1986). The same holds with higher errors for the samples of the

GVF (386 ± 159 and 325 ± 54 Ma). It is still unknown whether this hydrothermal overprint has to be regarded as a discrete event or rather represents the final stage in evolution of the Damara metamorphism.

The last episodic lead loss can probably be attributed to the break-up of Gondwana accompanied by an increased heat-flow in the crust (Haack, 1983) and/or uplift and erosion in the investigated area. This may have induced the partial resetting of the uranium rich (hence more corroded) zircons due to pressure release, possibly combined with hydrothermal activity (dilatancy model of Goldich & Mudrey, 1972). However, errors in the lower intercepts of samples GP8 and GP9, 49 ± 58 Ma and 55 +136 -145 Ma, are too high to definitely exclude anyone of these mechanisms for lead loss. From the neighbouring Rostock area, lower intercepts varying from 114 ± 9 to 221 ± 18 Ma were reported and interpreted as related to the break up of Gondwana by Pfurr *et al.* (1991).

Rb-Sr isotopic investigations

Due to the high error limits, the results of the Rb-Sr isotopic investigation do not constrain the comagmatic evolution of the WIC and the GVP. The large data scatter may firstly reflect the small variation in Rb/Sr ratios. Secondly, hybrid magmas composed of mantle and crustal materials could have caused variations in the $^{87}Sr/^{86}Sr$-initial ratios as a function of different mixing ratios and would not allow the construction of an isochron at all. Thirdly, the post-emplacement alteration which probably played an important role commonly results in rejuvenation of the isotope system (Hradetzky & Lippolt, 1993).

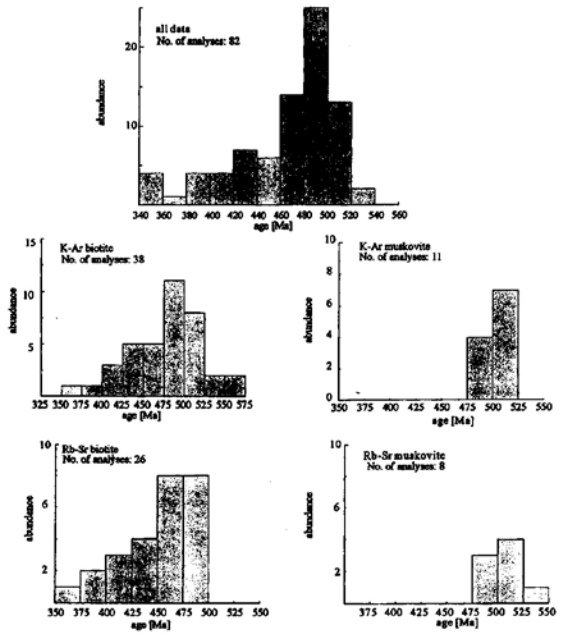

Figure 12: Histograms of Rb-Sr and K-Ar mica ages within the Southern Margin Zone and the Southern Foreland of the Damara Orogen (data compiled from Seifert, 1986, Pfurr, 1990, Ziegler & Stoessel, 1993)

The Rb-Sr errorchron age of 1653 ± 120 Ma for the WIC is considerably younger than the U-Pb zircon ages from this intrusion and therefore points to the third mechanism. Altogether, the data clearly indicate the different ages and origins of the WIC in the type locality and other granodioritic intrusions of Sinclair-age in the SMZ which were attributed to the Werner Intrusive Suite in the past (Reid *et al.*, 1988). In contrast, the Rb-Sr errorchron age of 1760 ± 123 Ma for the GVF coincides well with the zircon data of the WIC. However, the error limits are again too high to attest to a comagmatic evolution of both units.

In contrast to the WIC, no significant radiogenic Sr-loss has occurred in the GVF, provided the age obtained is the time of formation. This may result from dominant incorporation of Rb and Sr into the same mineral (i.e feldspar) whereas in the WIC these elements are concentrated in different minerals (i.e. biotite and feldspar) with variable susceptibility to alteration. If 1750 Ma is the approximate age of these units, the apparent difference in the Sr-initial ratios of the WIC and the GVF would be an artefact. Based on a 1750 Ma age, the recalculation of the $^{87}Sr/^{86}Sr$ isotope ratio of all samples shows there is no difference between the initials of both units (Fig. 13) with weighted mean $\varepsilon^{1750}_{UR}(Sr)$ values of 12.1 ± 17.2 (GVF) and 7.45 ± 10.0 (WIC).

For the WIC, almost all criteria point to classification as calc alkaline I-type magmatic rock: the A/CNK ratios vary from 0.83 to 1.08; K_2O/Na_2O ratio is always below unity; Na_2O concentrations in general exceed 3 wt.%; and the weighted mean $\varepsilon^{1750}_{UR}(Sr)$ of nine samples is low (Becker *et al.*, in prep.). This indicates an upper mantle or lower crustal origin of the magma, in accordance with the zircon typologies.

Conclusions

The results of the isotopic investigations suggest that formation of the pre-Rehoboth units and the Re-

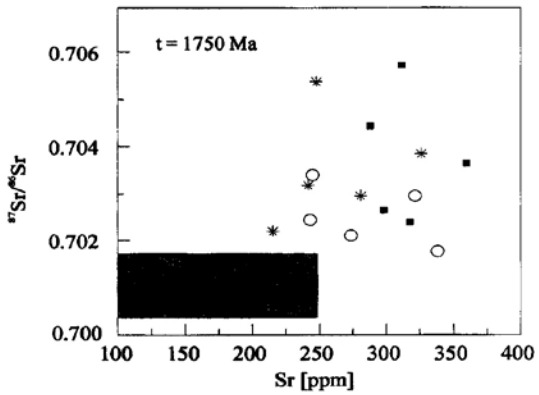

Figure 13: Recalculation of $^{87}Sr/^{86}Sr$ initial ratios at an assumed age of 1750 Ma

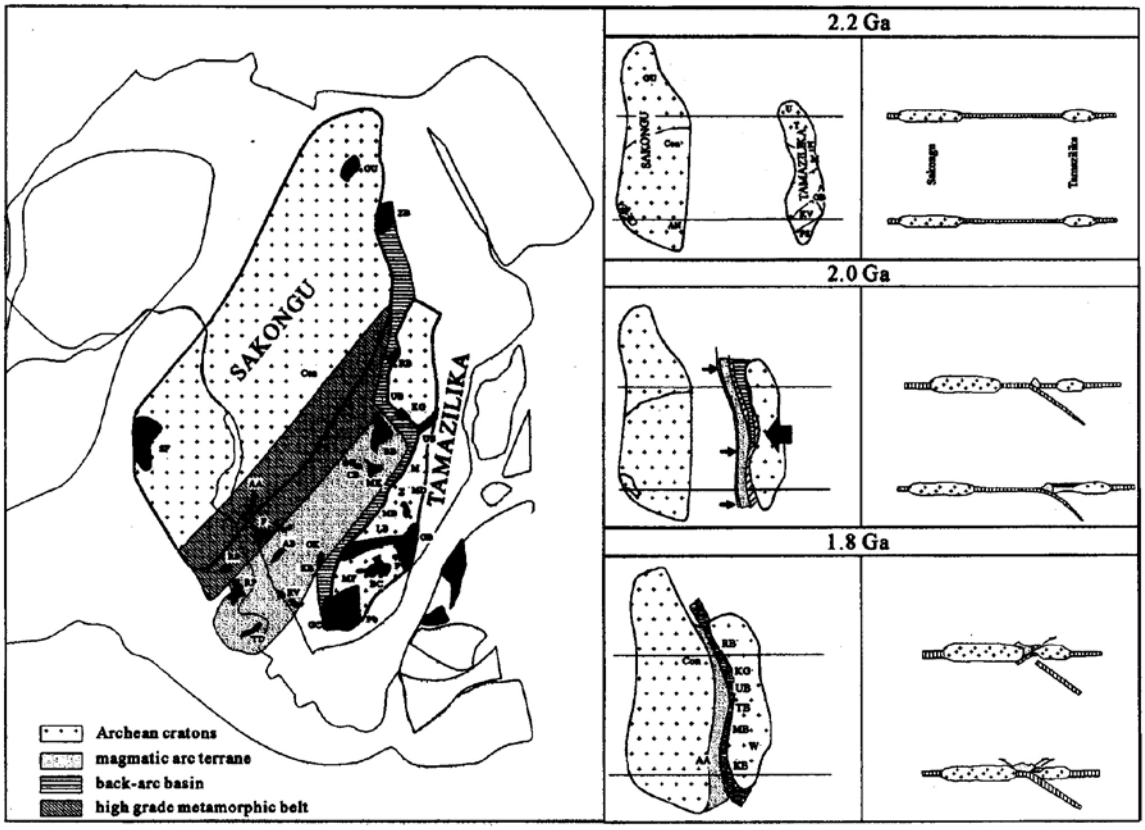

symbol	lithological unit	age	interpretation
AA	Angola Anorthosite	ca. 2.0 Ga	late orogenic intrusion
AB	Abbabis Inlier	ca. 2.0 Ga	magmatic arc
BB	Bangweulu Block	ca. 1.8 Ga	magmatic arc
BC	Bushveld Complex	ca. 2.0 Ga	cratonic layered intrusion (back-arc)
CB	Cooperbelt Basement	ca. 2.0 Ga	magmatic arc
CON	Congo Craton	>2.5 Ga	archaic craton (Sakongu)
F	Franzfontein Inlier	ca. 1.8 Ga	fore-arc basin + post-collisional granitoids
FR	Francevillian	ca. 2.0 Ga	passive continental margin
GB	Grunehogna Block	>2.5 Ga	archaic craton (Tamazilika)
GC	Gascoigne Belt	ca. 1.8 Ga	back-arc basin
GU	Gebel Uweinat	>2.5 Ga	archaic craton (Sakongu)
K	Kasai Craton	>2.5 Ga	archaic craton (Sakongu)
KB	Kheis Belt	ca. 2.0 Ga	back-arc basin
KG	Kapalagulu Complex	ca. 1.8 Ga	cratonic layered intrusion (back-arc)
LB	Limpopo Belt	> 2.5 Ga	archaic mobile belt
M	Malawi	ca. 2.0 Ga	back-arc basin
MB	Magondi Belt	ca. 2.0 Ga	back-arc basin
MD	Mashonaland Dolerites	ca. 1.9 Ga	cratonic dyke swarm (back-arc)
MF	Molopo Farms Complex	ca. 2.0 Ga	cratonic layered intrusion (back-arc)
MK	Mkushi	ca. 2.0 Ga	magmatic arc
MP	Marungu Plateau	ca. 1.8 Ga	magmatic arc (during back-arc closure)
OE	Oendelungu	ca. 2.0 Ga	fore-arc basin + post -collisional migmatites
P	Phalaborwa Complex	ca. 2.0 Ga	cratonic alkali complex (back-arc)
PS	Palala Shear Zone	ca. 1.9 Ga	reactivated structure
QF	Quadrilatero Ferriferro	ca. 2.0 Ga	passive continental margin
RB	Ruwenzori Belt	ca. 2.0 Ga	back-arc basin
RP	Rio de la Plata Craton	ca. 2.0 Ga	magmatic arcn + post-collisional migmatites
RS	Rio Grande do Sul	ca. 2.0 Ga	magmatic arc + post-collisional migmatites
RV	Richtersveld	ca. 2.0 Ga	magmatic arc
SF	Sao Francisco Craton	>2.5 Ga	archaic craton (Sakongu)
TB	Tumbide Belt	ca. 1.8 Ga	back-arc basin
TD	Tandilia	ca. 2.0 Ga	magmatic arc + post-collisional migmatites
UB	Ubendian Belt	ca. 1.8 Ga	back-arc basin
US	Usagaran Belt	ca. 1.8 Ga	aulakogen
W	Waterberg Basins	ca. 1.8 Ga	strike-slip basin (collisional stage)
Z	Zimbabwe Craton	>2.5 Ga	archaic craton (Tamazilika)
ZB	Zalingi Belt	ca. 2.0 Ga	back-arc basin ?

Figure 14: Plate tectonic model for the Eburnian orogeny (from Master, 1993).

hoboth Sequence occurred in a single major magmatic event approximately 1750 Ma ago. Similar ages have been obtained in crustal segments which extend from southern Brazil through southern Africa to equatorial Africa and constitute a major crust-forming event during Paleoproterozoic times (Eburnian-Ubendian cycle). A plate tectonic model for the evolution of this belt was first proposed by Master (1993). According to this model (Fig. 14), convergence of two late Archaean continents and southeastward subduction of oceanic crust occurred between 2.2 - 2.0 Ga, resulting in the formation of a magmatic arc and back arc on the leading plate in the south. At *ca.* 1.8 Ga ocean closure and collision ended in major orogenic deformation, high-grade metamorphis~ and collision related magmatism. A separate evolution is assumed for the northern part of this magmatic belt with a second stage of back arc opening and the formation of a magmatic arc which overprints the earlier *ca.* 2.0 Ga magmatic arc.

The isotopic ages obtained from granitoids of the Rehoboth Basement Inlier mostly spread between 1700-1860 Ma. Similar age data from other inliers in Namibia indicate widespread magmatism during this period and would point to formation of most of the magmatic rocks during the proposed collisional or post-collisional event (Table 2). However, geochemical data for the WIC and the GVF rather support an origin in a primitive magmatic arc or back arc setting (Becker, 1995). This is indicative of evolution of the RBI similar to the north of the proposed belt, with prolonged or renewed ocean opening and subduction related magmatism. The different metamorphic grade of units which are classified as pre-Rehoboth basement as compared to units of the Rehoboth Sequence may be explained by submersion to different crustal levels during subsequent thrust or extension tectonics.

Acknowledgements

This study was funded by the research grant AZ 1166/5.1 of the Deutsche Forschungsgemeinschaft (DFG). It was carried out as part of a University Research Project in cooperation with the Geological Survey of Namibia which supported the field work. A first draft was kindly corrected by H. Porada.

References

Barton, E.S. and Burger, A.J. 1983. Reconnaissance isotopic investigations in the Namaqua Mobile Belt and implications for Proterozoic crustal evolution-Upington geotraverse. *Spec. Publ. geol. Soc. S. Afr.*, **10**, 173-191.

Becker, T. 1995. Die Geologie, Geochemie und Altersstellung des Weener Igneous Komplex und der Gaub Valley Formation am Südrand des Damara Orogens, Namibia und ihre Bedeutung für die Genese der frühproterozoischen Rehoboth Sequenz. *Cuvillier Verlag, Göttingen*, 250 pp.

Becker, T., Ahrendt, H. and Weber, K. 1994. Report: the geological history of the Pre-Damaran Gaub Valley Formation and Weener Igneous Complex in the vicinity of Gamsberg. *Comm. Geol. Surv. Namibia*, **9**, 79-91.

Burger, A.J. and Coertze, F.J. 1976. Age determinations - April 1972 to March 1974. *Ann. geol. Surv. S. Afr.*, **10**, 135-142.

Burger, A.J. and Coertze, F.J. 1978. Summary of age determinations carried out during the period April 1974 to March 1975. *Ann. geol. Surv. S. Afr.*, **11**, 317-322.

Burger, A.J. and Walraven, F. 1978. Summary of age determinations carried out during the period April 197 5 to March 1976. *Ann. geol. Surv. S. Afr.*, **11**, 323-329.

Burger, A.J. and Walraven, F. 1979. Summary of age determinations carried out during the period April 1976 to March 1977. *Ann. geol. Surv. S. Afr.*, **12**, 415-431.

Crampton, D. 1974. A note on the age of the Matsap Formation of the northern Cape Province. *Trans. geol. Soc. S. Afr.*, **77**, 71-72.

De Carvalho, H. 1970. Contribution à la géo-chronologie du sudouest de l' Angola. *Bolm Servs. Geol. Min. Angola*, **19**, 23-35.

De Waal, S.A. 1966. *The Alberta Complex, a metamorphosed layered intrusion north of Nauchas, SWA: the surrounding granites and repeated folding in the younger Damara system*. D.Sc. Thesis, Univ. Pretoria (unpubl.), 203 pp.

Goldich, S.S. and Mudrich, M.G. 1972. Dilatancy model for discordant U-Pb zircon ages, 415-418. *In*: A.J. Tugarinov (ed.) *Contributions to Recent Geochemistry and Analytical Chemistry*. Moscow, Nauka Publ. Office, 654 pp.

Haack, U. 1983. Reconstruction of the cooling history of the Damara Orogen by correlation of radiometric ages with geography and altitude. *In*: H. Martin and F.W. Eder (eds.) *Intracontinental fold belts - Case studies in the Variscan Belt in Europe and the Damara Belt in Namibia*. Springer, Berlin, 945 pp.

Hill, R.S. 1975. Geological map 2315 BD-Rostock, scale 1:50000. *Geol. Surv. SWA/Namibia* (unpubl.).

Hradetzky, H. and Lippolt, H.J. 1993. Generation and distortion of Rb/Sr whole-rock isochrons - effects of metamorphism and alteration. *Eur. J. Mineral.*, **5**, 1175-1193.

Hugo, P.J. and Schalk, K.E.L. 1972. The isotopic ages of certain granites and acid lavas in the Rehoboth and Maltahohe Districts, SWA. *Ann. geol. Surv. S. Afr.*, **9**, 103-105.

Jacob, R.E., Kröner, A and Burger, A.J. 1978. Areal extent and first U-Pb age of the pre-Damaran Abbabis Complex in the central Damara belt of South West Africa/Namibia. *Geol. Rundsch.*, **67**, 706-718.

Krogh, T.E. 1973. A low contamination method for hy-

drothermal decomposition of zircon and extraction of U and Pb for isotopic age determinations. *Geochim. Cosmochim. Acta*, **37**, 485-494.

Ludwig, K.R. 1980. Calculation of uncertainties of U-Pb isotope data. *Earth Plan. Sci. Let.*, **46**, 212-220.

Ludwig, K.R. and Stuckless, J.S. 1978. Uranium-lead isotope systematics and apparent ages of zircons and other minerals in Precambrian granitic rocks, Granite mountains, Wyoming. *Contr. Mineral. Petrol.*, **65**, 243-254.

Master, S. 1990. The "Ubendian" cycle in equatorial and southern Africa: accretionary tectonics and continental growth. *In*: Rocci, G. and Deschamps, M. (eds.) *New data in African earth sciences.* 15th Coll. Afr. Geol., Orleans, CIFEG Occ. Publ., **22**, 41-44.

Master, S. 1993. Early Proterozoic assembly of "Ubendia" (Equatorial and Southern Africa and adjacent parts of South America): tectonic and metallogenic implications. Symposium Early Proterozoic, Geochemical and Structural constraints - metallogeny, *CIFEG Occ. Publ.* **23***, Dakar*, 103-107.

Nagel, R., Warkus, F., Becker, T. and Hansen, B.T. 1996. U/Pb-Zirkondatierungen der Gaub Valley Formation am Südrand des Damara Orogens, Namibia, und ihre Bedeutung für die Entwicklung des Rehoboth Inlier. *Z. Geol. Wiss.*, **24** (5), 611-618

Pfurr, N. 1990. *Die Altersstellung von Rotgneisen im Rostock Deckenkomplex am Südrand des Damara Orogens, Namibia, abgeleitet aus U/Pb- und Rb/Sr-Isotopenuntersuchungen, und ihre Bedeutung für die Basement-Cover-Beziehungen in der Damara Südrandzone*. Dr. rer. nat. thesis (unpubl.) Univ. Göttingen, 179 pp.

Pfurr, N., Ahrendt, H., Hansen, B.T. and Weber, K. 1991. U-Pb and Rb-Sr isotopic study of granitic gneisses and associated metavolcanic rocks from the Rostock massif, southern margin of the Damara Orogen: implications for lithostratigraphy of this crustal segment. *Comm. geol. Surv. Namibia*, **7**, 35-48.

Pupin, J.P. 1980. Zircon and Granite Petrology. *Contr. Mineral. Petrol.*, **73**, 207-220.

Reid, D.L., MaIling, S. and Allsopp, H.L. 1988. Rb-Sr ages of granitoids in the Rehoboth-Nauchas area SWA Namibia. *Comm. geol. Surv. SWA/Namibia*, **4**, 19-28.

Schalk, K.E.L. 1988. Pre-Damaran basement rocks in the Rehoboth and southern Windhoek districts (areas 2217D, 2316, 2317A-C) - a regional description. *Unpubl. Rep. geol. Surv. SWA, Windhoek*.

Schulze-Hulbe, A. 1979. Pre-Damaran Formations on Marienhof 577, Aroams 315, Doornboom 316 and Gollschau 20, Areas 2316BC and BD, Rehoboth district. *Unpubl. Rep. geol. Surv. SWA, Windhoek*.

Seifert, N. 1986. Geochronologie am Sudrand des Damara Orogen, SWA/Namibia: hydrothermale beeinflussung von Isotopensystemen und Abkuhlalter in prakambrischen basementgesteinen. *Schweiz. miner. petro gr. Mitt.*, **66**, 413-451.

South African Committee For Stratigraphy (SACS) 1980. Stratigraphy of South Africa, South West Africa/Namibia and the Republics of Bophuthatswana, Transkei and Venda. *Hand. geol. Surv. S. Afr.*, **8**, 690 pp.

Stacey, J.S. and Kramers, J.D. 1975. Approximation of terrestrial lead isotope evolution by a two stage model. *Earth Plan. Sci. Let.,* **26**, 207-221.

Steiger, R.H. and Jäger, E. 1977. Subcommission on geochronology: Convention on the use of decay constants in geo- and cosmochronology. *Earth Plan. Sci. Let.*, **36**, 359-362.

Tegtmaier A. and Kröner, A. 1985. U-Pb zircon ages for the granitoid gneisses in Northern Namibia and their significance for Proterozoic crustal evolution of Southwestern Africa. *Precamb. Res.*, **28**, 311-328.

Teufel, S. 1988. Vergleichende U/Pb- und Rb-Sr-altersbestimmungen an gesteinen des übergangsbereiches Saxothuringikum/Moldanubikum, NE Bayern. *Göttinger Arb. Geol. Pal.*, **35**, 87 pp.

Watters B.R 1976. Possible late Precambrian subduction zone in South West Africa. *Nature,* London. **259**, 471-473.

Wetherill, G.S. 1956. Discordant uranium-lead ages. *J. Trans. Am. Geophys. Union*, **37**, 320-326.

York, D. 1969. Least-squares fitting of a straight line with correlated errors. *Earth Plan. Sci. Let.*, **5**, 320-324.

Ziegler, D.RF. and Stoessel, G.F.U. 1991. Isotope geology and geochemistry of the Rehoboth Basement Inlier, Namibia/SWA; a multimethod case history. *Bull. Swiss. Assoc. of Petroleum Geol. & Eng.*, **56**, 13-33.

Ziegler, U.R.F. and Stoessel, G.F.U. 1992. Note: New constraints on the age of the Weener Intrusive Suite, the Gamsberg Granite and the crustal evolution of the Rehoboth Basement Inlier, Namibia. *Comm. geol. Surv. SWA/Namibia*, **7**, 75-78.

Ziegler, D.R.F and Stoessel, G.F.D. 1993. Age determinations in the Rehoboth Basement Inlier, Namibia. *Mem. Geol. Surv. Namibia*, **14**, 106 pp.